Translational Oncology
www.transonc.com

Volume 2 Number 3 September 2009 pp. 164–173 164

Combination of Enzastaurin and Pemetrexed Inhibits Cell Growth and Induces Apoptosis of Chemoresistant Ovarian Cancer Cells Regulating Extracellular Signal–Regulated Kinase 1/2 Phosphorylation[1,2]

Karen Bräutigam*,†, Dirk Olaf Bauerschlag*,‡, Marion Tina Weigel*, Julia Biernath-Wüpping*, Thomas Bauknecht[§], Norbert Arnold*, Nicolai Maass*,‡ and Ivo Meinhold-Heerlein*,‡

*Department of Gynecology and Obstetrics, University Hospital Schleswig-Holstein, Kiel, Germany; †Burnham Institute for Medical Research, La Jolla, CA, USA; ‡Department of Gynecology and Obstetrics, University Hospital Aachen, Aachen, Germany; §Medical-Oncology, Lilly Deutschland GmbH, Bad Homburg, Germany

Abstract

New strategies in the therapy for malignant diseases depend on a targeted influence on signal transduction pathways that regulate proliferation, cell growth, differentiation, and apoptosis by the activation of serine/threonine kinases. Enzastaurin (LY317615.HCl), a selective inhibitor of protein kinase Cβ (PKCβ), is one of these new drugs and causes inhibition of proliferation and induction of apoptosis. Pemetrexed, a multitarget inhibitor of folate pathways, is broadly active in a wide variety of solid tumors. Therefore, the effect of enzastaurin and the combination treatment with pemetrexed was analyzed when applied to the drug-sensitive ovarian cancer cell line HEY and various subclones with drug resistance against cisplatin, etoposide, docetaxel, and paclitaxel, as well as pemetrexed, and gemcitabine. In these novel chemoresistant subclones, the expression of the enzastaurin targets PKCβII and glycogen synthase kinase 3β (GSK3β) was analyzed. Exposition to enzastaurin showed various inhibitory effects on phosphorylated forms of GSK3β and the mitogen-activated protein kinase extracellular signal–regulated kinase 1/2. Cell proliferation experiments identified the cell line–specific half-maximal inhibitory concentration values of enzastaurin and a synergistic inhibitory effect by cotreatment with the antifolate pemetrexed. Induction of apoptosis by enzastaurin treatment was investigated by Cell Death Detection ELISA and immunoblot analyses. Simultaneous treatment with pemetrexed resulted in an enhanced inhibition of proliferation and induction of apoptosis even in partial enzastaurin-resistant cells. Therefore, the combinational effect of enzastaurin and pemetrexed can have promise in clinical application to overcome the fast-growing development of resistance to chemotherapy in ovarian cancer.

Translational Oncology (2009) 2, 164–173

Introduction

Ovarian cancer accounts for the highest tumor-related mortality among women whose conditions were diagnosed with gynecologic malignancy. Although the incidence of 21,650 new cases accounts for only 3% of all female cancers, 15,520 patients in the United States are predicted to die of ovarian cancer in 2008, as estimated by the American Cancer Society [1]. This high ratio of death to incidence is mostly due to late-stage diagnosis caused by minimal and rather unspecific symptoms. The poor prognosis of advanced stage ovarian cancer is reflected in a 5-year survival rate of less than 30% for patients diagnosed with FIGO stage III or IV disease [2]. Cytoreductive surgery is one of the most important prognostic factors in ovarian cancer [3], and adjuvant chemotherapy with a combination of carboplatin and paclitaxel is considered the

Address all correspondence to: Karen Braeutigam, Burnham Institute for Medical Research, 10901 N Torrey Pines Rd, La Jolla, CA 92037. E-mail: karenbraeutigam@gmx.de

[1]The authors thank the unrestricted research grant from Lilly GmbH Deutschland that supported this study.

[2]This article refers to supplementary materials, which are designated by Table W1 and Figures W1 and W2 and are available online at www.transonc.com.

Received 17 February 2009; Revised 1 April 2009; Accepted 7 April 2009

DOI 10.1593/tlo.09121

criterion standard [4]. Although this is a potent combination, many patients experience a recurrence within 6 months of the last cycle of chemotherapy. These prognostically unfavorable early relapses are presumed to be platinum- and taxane-resistant and associated with only short-term survival. Thus, overcoming chemotherapy resistance remains a key problem in the treatment of advanced ovarian cancer, and consequently, new drugs targeting cancer-specific molecules are needed.

In cancer cells, the balance between apoptosis and cell proliferation is adjusted in favor of cell growth. Protein kinases C (PKCs) are a family of serine/threonine kinases comprising at least 12 isoforms that are involved in tumor formation and progression [5,6]. Several reports have shown that activation of PKC is required for tumor-induced angiogenesis [7,8]. In addition, PKC activation triggers signaling through the ras/extracellular signal–regulated kinase 1/2 (ERK1/2) pathway, which may be involved in the controlling of cellular proliferation and apoptosis [9–11] as well as the induction of intestinal cell invasiveness [12]. Protein kinase C activation requires the activity of phosphatidylinositol-dependent kinase 1, a key effector kinase, activated immediately downstream of the phosphatidylinositol 3-kinase (PI3K), which gives rise to a link between the activities of PKC and PI3K/AKT pathway, a prominent regulatory pathway governing the apoptotic response [13]. Further evidence for overlapping signaling pathways is the direct phosphorylation of AKT at Ser^{473} by PKCα, PKCβ, and PKCη [14–16]. Moreover, both PKC and AKT can phosphorylate glycogen synthase kinase 3β at Ser^{9} (GSK3β) [17–19]. Cross talk between PKC and the PI3K/AKT pathway may be an attractive mechanism by which PKCs influence the apoptotic response. Furthermore, the resistance of cancer cells to treatment can be attributed in many instances to activation of intracellular signaling pathways involved in survival, such as the Ras-Raf-MEK-ERK1/2 or the PI3K/AKT pathway [20].

The contribution of PKCs in tumor progression initiates the development of novel anticancer therapeutics targeting PKC. Enzastaurin (LY317615.HCl; Eli Lilly and Company, Indianapolis, IN), an acyclic bisindolylmaleimide, was developed as a potent and selective ATP competitive inhibitor of PKCβ [21]. Enzastaurin has shown to be antiapoptotic and antiproliferative in tumor cells *in vitro* and demonstrated *in vivo* efficacy in small cell lung, colon, renal, glioma, and multiple myeloma tumor animal models [22–24]. The mechanisms of action leading to tumor suppression *in vivo* seem to be complex. In addition to PKC inhibition, enzastaurin impedes the PI3K/AKT pathway, as evaluated by the inhibition of GSK3β and AKT phosphorylation in tumor cells and tumor tissue [23,25].

The aim of our investigation was to evaluate whether enzastaurin can cause apoptosis and growth inhibition of chemotherapy-resistant ovarian cancer cell lines. Using the parental HEY cell line, subclones were developed with selective resistance against cisplatin, etoposide, docetaxel, paclitaxel, pemetrexed, gemcitabine, and enzastaurin as control cell line, respectively. Inhibition of proliferation and induction of apoptosis were examined in all analyzed cell lines. Because we observed only partial inhibition of proliferation at clinically achievable concentrations [26], we also questioned whether therapeutic efficacy could be enhanced by a combination treatment with pemetrexed. Pemetrexed (Alimta; Eli Lilly and Company) is a novel multitargeted antifolate that potently inhibits thymidylate synthase and, to a much lesser extent, glycinamide ribonucleotide formyltransferase and dihydrofolate reductase, thus directly decreasing the growth rate of tumor cells by limiting the available pools of thymidine required for DNA synthesis [27]. Pemetrexed induces apoptosis in a broad spectrum of solid tumors, including breast, colorectal, gastric, cervical, bladder, and non–small cell lung cancer (NSCLC) [28]. Furthermore, it has been associated with a significant reduction of phosphorylated AKT as well as a synergistic antiproliferative effect in combination treatment with gemcitabine in human NSCLC cells [29]. Pemetrexed has also shown clinically relevant activity in combination with other chemotherapeutic agents such as gemcitabine in solid tumors, including ovarian cancer [30,31].

Materials and Methods

Drugs and Antibodies

Enzastaurin (10 mM stock aliquots in DMSO at −20°C), pemetrexed, and gemcitabine (100 mM stock aliquots in PBS at −20°C) were obtained from Eli Lilly. Cisplatin, etoposide, docetaxel, and paclitaxel were purchased from Sigma (Taufkirchen, Germany) and stored as recommended by the manufacturer. Primary antibodies were obtained from New England Biolabs [Frankfurt am Main, Germany; phospho-GSK3β (Ser^{9}), phospho-AKT (Ser^{473}), AKT, phospho-ERK1/2 (Thr^{202}/Tyr^{204}), ERK1/2, caspase 8, caspase 9, poly(ADP-ribose) polymerase (PARP)], BD Biosciences (Heidelberg, Germany; GSK3β), and Sigma (β-actin). Secondary, either antimouse or antirabbit, antibodies were purchased from GE Healthcare (München, Germany).

Cell Culture and Cytostatic Drug Resistance Cultivation

The parental ovarian cancer cell line HEY emanated from ascites cells of a moderately differentiated serous papillary ovarian carcinoma and served as origin for cultivation of the cytostatic drug-resistant subpopulations. Cells were treated three times a week with increasing concentrations of the subsequent cytostatic drugs (median duration, 8-10 months) until the cells exhibited significant resistance. Long-term cultivation was done with growth media RPMI 1640 (Biochrom, Berlin, Germany) containing 2.0 g/L $NaHCO_3$, stable glutamine, 10% fetal calf serum (Invitrogen, Karlsruhe, Germany), 50 U/ml penicillin (Biochrom), and 50 mg/ml streptomycin (Biochrom) at 37°C and 5% CO_2. The appropriate cytostatic drug for each of the resistant subclones was additionally supplied (2 μg/ml cisplatin, 5 μg/ml etoposide, 15 ng/ml docetaxel, 40 ng/ml paclitaxel, 3 μM pemetrexed, 5 μM gemcitabine, and 25 μM enzastaurin). Resistance was proven by MTS Assay from Promega (Mannheim, Germany; Table W1). Stimulation experiments for immunoblot analyses were performed under serum-starved conditions.

Cell Proliferation Assay

Inhibition of proliferation was determined with a colorimetric MTS (3-[4,5-dimethylthiazol-2yl]-5-[3-carboxymethoxyphenyl]-2-[4-sulfophenyl]-2*H* tetrazolium) cell proliferation assay (CellTiter96 Aqueous Non-Radioactive Cell Proliferation Assay; Promega). Five thousand cells were seeded in 96-well microtiter plates (Sarstedt, Nümbrecht, Germany) in 200 μl of growth medium. After an overnight attachment period, cells were exposed for 72 hours at 37°C and 5% CO_2 to various concentrations of enzastaurin (0.625-40 μM) and, in subsequent experiments, to denoted concentrations of enzastaurin and pemetrexed (10 and 50 nM), alone and in combination. Control cells received vehicle alone (0.4% DMSO). After the 72 hours of treatment, media were exchanged and 20 μl of Assay reagent was added to each well. After incubation for an additional 2 hours, the number of viable cells was determined by measuring the absorption of the generated formazan spectrophotometrically at 490 nm. The proliferation inhibition was indicated by the percentage

of absorption of sample and control wells. All studies were performed in triplicate and repeated at least three times independently. To calculate half-maximal inhibitory concentration (IC_{50}) values, the drug concentration data, x_1, x_2, …, x_n, were logarithm-transformed and the growth inhibition data, y_1, y_2, …, y_n, were in the range of 0 to 1. The IC_{50} values were estimated by plotting *x*-*y* and then fit the data with a straight line after the *x*-axis is logarithm-transformed [$Y = aX + b$; $IC_{50} = (0.5 - b) / a$].

Cell Death Detection ELISA

To investigate apoptosis induced by enzastaurin treatment, the Cell Death Detection ELISA (CDDE) plus (Roche, Mannheim, Germany), a sandwich enzyme immunoassay for detection of nucleosomes released during apoptotic process, was performed. Cells (5×10^3 per well) were disseminated in 96-well microtiter plates (Sarstedt) in 200 µl of growth medium. After an overnight attachment period, cells were treated with 1, 2, and 10 µM of enzastaurin for 24 hours at 37°C. After accomplishing the ELISA procedure, as recommended by manufacturer, release of nucleosomes was determined by measuring the absorption spectrophotometrically at 405 nm. Accumulation of the detached mononucleosomes and oligonucleosomes into the cytoplasm was calculated as enrichment factor (absorbance of sample/absorbance of corresponding negative control). Assay was performed in duplicate and repeated twice.

GSK3β ELISA

The decrease of activated GSK3β by enzastaurin treatment in cell lysates was determined with the DuoSet IC ELISA from R&D Systems (Wiesbaden, Germany), containing the basic components required for the development of sandwich ELISA to measure phosphorylated GSK3β. Both untreated cells and cells exposed to 5 µM enzastaurin were solubilized for different times (0.5-3 hours) in lysis buffer, 1 mM EDTA, 0.5% Triton X-100, 5 mM NaF, 1 M urea, 1% Protease Inhibitor Cocktail II (Sigma), and 1% phosphatase inhibitor. One microgram of total protein was used for the ELISA, which was performed as recommended by the manufacturer. Results were calculated by the mean of duplicates of samples and standards subtracted by the average zero standard.

Immunoblot Analysis

Total cell lysates were prepared and analyzed by immunoblot analysis. Cells, 1 to 5×10^6, were seeded in 10-ml culture dishes and incubated overnight at 37°C and 5% CO_2. Both untreated cells and cells treated with 5 and 10 µM enzastaurin, respectively, were solubilized for indicated times (0.5-48 hours) in lysis buffer containing 1 mM EDTA, 0.5% Triton X-100, 5 mM NaF, 1 M urea, 1% Protease Inhibitor Cocktail II, and 1% phosphatase inhibitor (Sigma). Vortexed samples were allowed to sit on ice for 1 hour, and sample protein concentrations were then quantified using a total protein assay (Bio-Rad, München, Germany). Equal amounts of protein were separated by SDS-PAGE and electrotransferred onto a polyvinylidene fluoride membrane (GE Healthcare). Membranes were blocked and incubated overnight with antibodies according to the manufacturer's recommendations. The proteins were visualized by enhanced chemiluminescence (ECL Plus Reagent; GE Healthcare). In addition, membranes were reprobed with antibodies against β-actin to ensure equal loading and transfer of proteins.

Results

Enzastaurin Treatment Suppresses Proliferation and Induces Apoptosis in the Parental and Cytostatic-Resistant Ovarian Cancer Cell Lines

To determine the effect of enzastaurin on the parental ovarian cancer cell line HEY and its drug-resistant counterparts, cells were cultured with increasing concentrations of enzastaurin (0.63-40 µM) for 72 hours, which resulted in a dose-dependent inhibition of proliferation in all examined cell lines. The cisplatin-resistant cell line was the only cytostatic-resistant cell line that exhibited stronger sensitivity to enzastaurin treatment than the parental HEY cells. Among the remaining cytostatic-resistant HEYs, the docetaxel-resistant cell line displayed the highest resistance to enzastaurin stimulation except for the enzastaurin-resistant control cell line, as also indicated in the table (Figure 1*A*).

To determine whether enzastaurin might induce apoptosis in our ovarian cancer cell lines, we performed the CDDE. As measured by oligonucleosomal fragmentation, a concentration of 10 µM enzastaurin significantly induced apoptosis mainly in cisplatin-resistant and parental HEYs and also, to a lesser extent, in the etoposide- and paclitaxel-resistant cell lines. Docetaxel-, pemetrexed-, and gemcitabine-resistant cells showed only a slight increase of enrichment factor indicating that enzastaurin stimulation caused nearly no apoptosis after 24 hours in these cells (Figure 1*B*).

Decreased Phosphorylation of GSK3β Correlates with Responsiveness to Enzastaurin

In the following investigation, we sought to examine an effect of enzastaurin on GSK3β phosphorylation in the cytostatic-resistant HEYs compared with the parental ones. Already after 30 minutes of treatment with 5 µM enzastaurin, a broad decrease of phosphorylated GSK3β in all examined HEY cells was observed which arose again after 3 hours of treatment (Figure 2). The expression pattern of phosphorylated GSK3β was very different within the untreated cells. The strongest expression of activated GSK3β was displayed by the cisplatin- and paclitaxel-resistant cell lines, whereas the parental HEYs showed a low protein level of phosphorylated GSK3β. Therefore, a correlation between the sensitivity for enzastaurin and the expression level of activated GSK3β failed (Figure 2*A*). In contrast, the enzastaurin-dependent dephosphorylation seems to correspond to the response to enzastaurin treatment as demonstrated by the percentages of enzastaurin-dependent decrease of phosphorylated GSK3β (Figure 2*C*). Here, the strongest dephosphorylation occurred in the parental and cisplatin-resistant HEYs, which are known to be more responsive to enzastaurin than the others. To confirm these ELISA-based results and validate a real dephosphorylation, immunoblot analyses were performed, which reflected the results very well (Figure 2*B*). The detection of total GSK3β with nearly identical band intensity within each cell line indicated that a real dephosphorylation occurred dependent on enzastaurin treatment. This was additionally validated by the expression analyses of β-actin.

Enzastaurin Shows a Slight Effect on AKT Phosphorylation in the Parental HEY Cell Line, and Causes Strong Variations in Phosphorylation of the Mitogen-Activated Protein Kinase ERK1/2

Treatment of the various HEY cell lines under identical conditions as for GSK3β expression—stimulation with 5 µM enzastaurin up to

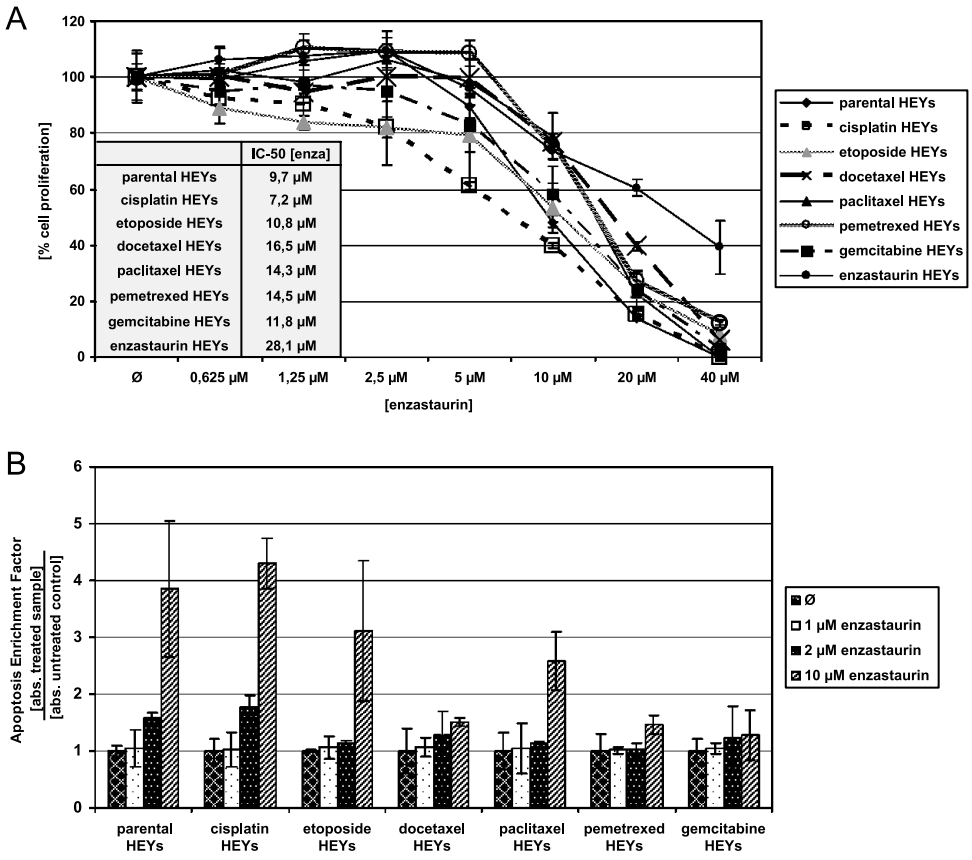

Figure 1. (A) Dose-dependent inhibition of proliferation due to enzastaurin treatment. Five thousand cells were seeded in 96-well plates and incubated for 72 hours with rising concentrations of enzastaurin, as indicated. MTS assay was performed as described in the Materials and Methods section. The parental and various drug-resistant HEYs showed enzastaurin-caused growth inhibition to a certain extent as indicated by the IC_{50} values in the table. (B) CDDE validates enzastaurin-induced apoptosis in parental and chemoresistant HEYs. Cells were treated with indicated enzastaurin concentrations for 24 hours, and CDDE was performed, as described in the Materials and Methods section.

3 hours—failed to inhibit AKT activity as detected by immunoblot experiment with phospho-AKT antibody (data not shown). Therefore, we checked the inhibition of phosphorylated AKT expression in parental HEY cells treated with 10 µM enzastaurin for 3, 6, 12, 24, and 48 hours and could observe a distinct decrease of phosphorylated AKT after 48 hours of enzastaurin exposition (Figure 3).

The adjacent analysis dealt with enzastaurin affecting the ERK1/2 pathway after treatment with 10 µM enzastaurin for analogous times in the parental HEY cell line. We could prove an alternating phosphorylation pattern as already demonstrated for GSK3β. A decline of phosphorylated ERK occurred after 3 hours with enzastaurin treatment, which rose again after 6 hours. A strong decrease was displayed after 12 hours of exposition, which increased again after an additional 12 hours, but declined nearly completely after 48 hours (Figure 3).

Combined Exposure of Ovarian Cancer Cell Lines to Enzastaurin and Pemetrexed Enhances Antiproliferative Effects

Because enzastaurin only partially inhibited the proliferation of parental and cytostatic-resistant HEY cell lines at clinically achievable concentrations, we questioned whether antiproliferative effects could be potentiated by the administration of an additional cytostatic drug that affects targets involved in PKC-mediated signaling. Cells were treated with various concentrations of enzastaurin with or without both 10 and 50 nM pemetrexed for 72 hours, and cell proliferation was measured with an MTS assay. The most promising result was achieved by the combination treatment of 5 µM enzastaurin plus 50 nM pemetrexed. Compared with the single treatment with either enzastaurin or pemetrexed, we could prove a synergistic proliferation inhibition effect by combined treatment in all examined cell lines, with the expected exception of the pemetrexed-resistant cells (Figure 4). The docetaxel-resistant HEYs, which were affected by neither 5 µM enzastaurin nor 50 nM pemetrexed, showed 50% less proliferating cells after the combination treatment. More than 30% of the etoposide-resistant cells, which did not respond to the single agents, were inhibited by enzastaurin in combination with pemetrexed. Although both inhibitors were effective with cisplatin-resistant cells on their own, combined exposition increased inhibition by another 30%. In the parental, the paclitaxel-resistant, and gemcitabine-resistant HEYs, not only that 50 nM pemetrexed caused proliferation inhibition as a single agent but also that a slight synergistic effect could be observed by the combination treatment. The enzastaurin-resistant cells responded strongly to pemetrexed alone, and surprisingly, both drugs caused a slight but even stronger proliferation inhibition. These results indicate that cotreatment with pemetrexed exhibits synergistic inhibitory effects on proliferation in ovarian cancer cell lines resistant against clinically established chemotherapeutics with the most promising effect in the docetaxel-resistant HEYs.

Pemetrexed Increases Enzastaurin-Induced Induction of Apoptosis and Inhibition of Proproliferative Kinases

We could also show that costimulation of pemetrexed increases apoptosis induced by enzastaurin. HEY cells were treated either with 10 μM enzastaurin or concomitantly with 10 μM enzastaurin plus 50 nM pemetrexed for 3, 6, 12, 24, and 48 hours. General apoptosis induction was proven by PARP cleavage, induction of the extrinsic apoptotic pathway by caspase 8 and induction of the intrinsic mitochondrial pathway by caspase 9 cleavage using immunoblot analyses. Partial PARP cleavage occurred after 48 hours of enzastaurin treatment. Combined treatment with pemetrexed resulted in nearly completely cleaved PARP, demonstrating increased induction of apoptosis. Investigation of the initiator caspases 8 and 9 also displayed a slight cleavage into the proapoptotic active proteins by enzastaurin stimulation, which was additionally enforced by concomitant administration of pemetrexed (Figure 5).

Subsequent immunoblot experiments were performed to determine an influence on the enzastaurin-caused dephosphorylation of GSK3β, AKT, and ERK. Treatment of the HEY cells was done with 10 μM enzastaurin alone and in combination with 50 nM pemetrexed for 3, 6, 12, 24, and 48 hours. Dephosphorylation of GSK3β was existent in all enzastaurin-treated samples compared with the untreated cells. Furthermore, we could demonstrate very strong dephosphorylation of GSK3β after 12 hours of enzastaurin exposition, which is consistent with the observation identified for the phosphorylation pattern of the mitogen-activated protein (MAP) kinase ERK. Cotreatment of pemetrexed resulted in a slightly stronger dephosphorylation of GSK3β after 6 hours but did not affect enzastaurin-caused dephosphorylation at other time points. Whereas cotreatment up to 12 hours demonstrated no additional effect on the phosphorylation of AKT, the combined treatment for 24 and 48 hours caused a stronger dephosphorylation of AKT compared with enzastaurin treatment alone. The enzastaurin-dependent

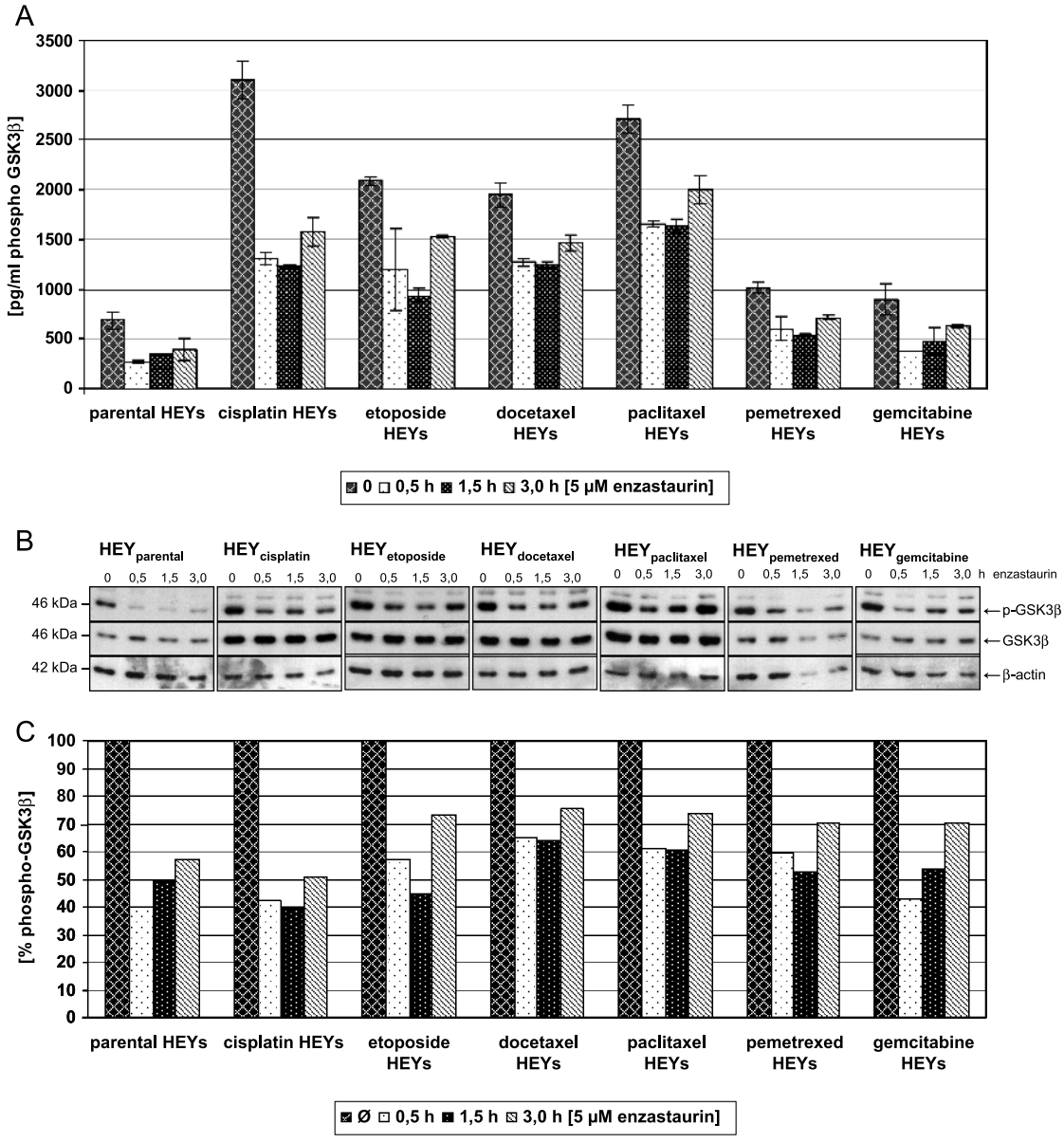

Figure 2. Effect of enzastaurin treatment on expression pattern of phosphorylated GSK3β in parental and drug-resistant HEY cell lines was determined by DuoSet ELISA (A) and immunoblot (B) analyses as described in the Materials and Methods section. (C) Relative percentages of enzastaurin-dependent decrease of phosphorylated GSK3β in the parental and chemoresistant HEY subclones.

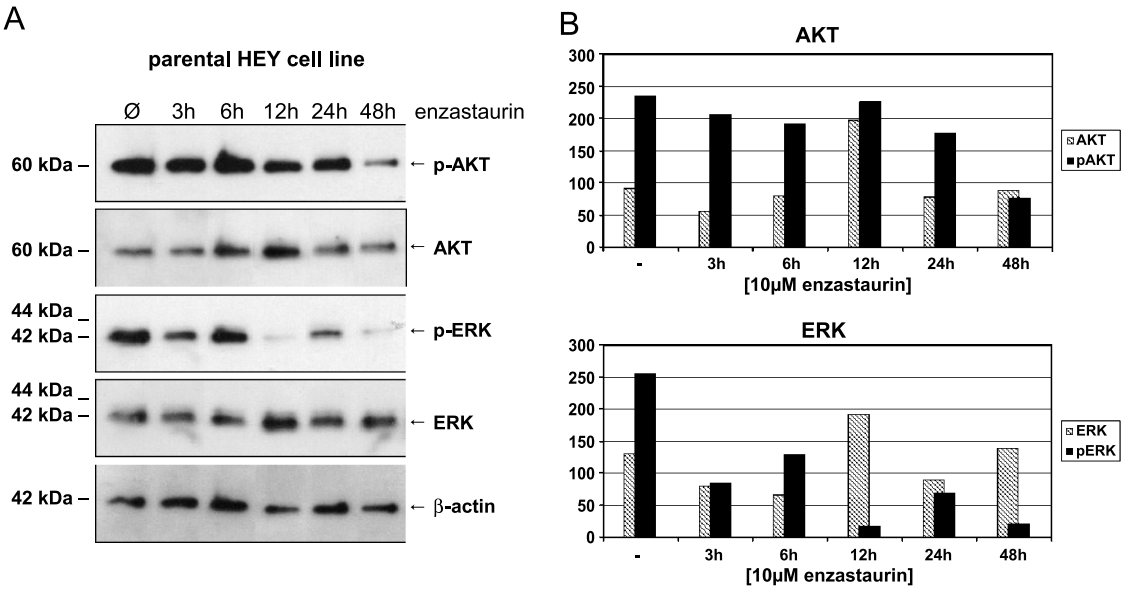

Figure 3. Effects of enzastaurin on AKT and the MAP kinase ERK1/2. (A) Parental HEY cells were treated with 10 μM enzastaurin for indicated times, and both phosphorylated and total amount of protein expression were determined by immunoblot experiments with the appropriate antibodies. Expression analysis of β-actin served as loading control. (B) Histograms show densitometrical analyses of the phosphorylated and total amount of the protein expression of AKT and the MAP kinase ERK1/2 normalized to the protein expression of β-actin.

dephosphorylation of the MAP kinase ERK was also further decreased by addition of pemetrexed after 48 hours of treatment (Figure 6).

Discussion

The biggest problem in the treatment of ovarian cancer is the fast-emerging resistance against currently applied drugs (mainly platinum and taxane derivates) observed in patients. In the recent past, great efforts have been made to develop new molecular therapies to potentiate the effectiveness of current cytostatic drugs and to overcome chemotherapy resistance. Many of these new drugs affect signaling pathways that interfere with the induction of apoptosis and inhibition of proliferation. PKC activity has been implicated in the regulation of tumor-induced angiogenesis, tumor cell proliferation, and tumor invasiveness. Enzastaurin, an ATP-competitive, selective inhibitor of PKCβ, was shown to exhibit a direct effect on human tumor cells, inducing apoptosis in, and suppressing proliferation of, a wide array of cultured human tumor cells. Enzastaurin treatment was reported to interfere with signaling through the AKT pathway, suppressing phosphorylation of GSK3β in various tumor cells, for example, human glioma cells [32] and human xenograft tissues [23], suggesting that GSK3β phosphorylation may serve as a reliable pharmacodynamic marker of enzastaurin activity. In our investigation, we could demonstrate a dose-dependent inhibition of proliferation in the parental ovarian carcinoma cell line HEY and in the subclones with resistance against cisplatin, etoposide, docetaxel, paclitaxel, pemetrexed, and gemcitabine, respectively, after

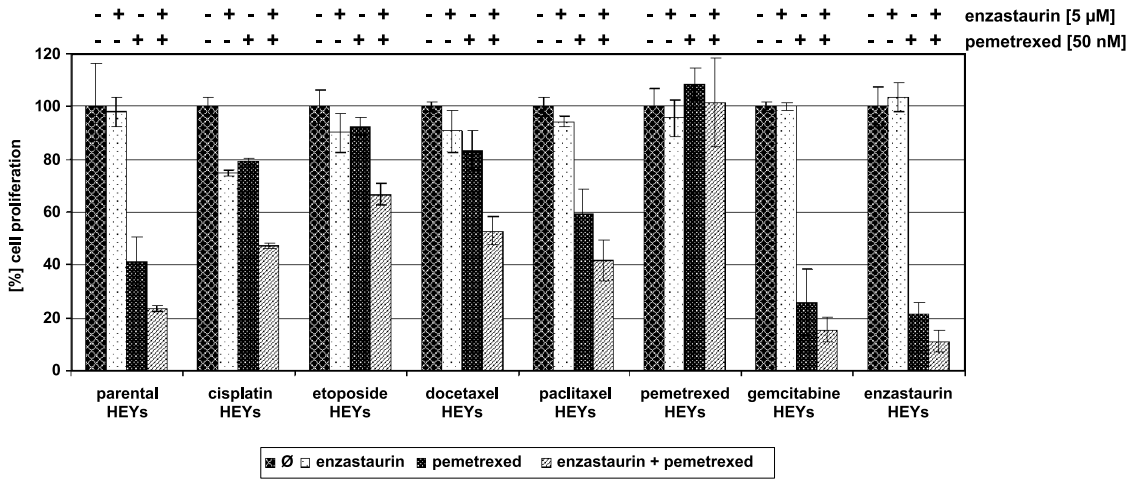

Figure 4. Cotreatment of pemetrexed and enzastaurin exhibited synergistically antiproliferative effects on parental and chemoresistant HEY cell lines. Investigation of single and concomitant stimulation with 5 μM enzastaurin and 50 nM pemetrexed for 72 hours was done by MTS assay as described in the Materials and Methods section.

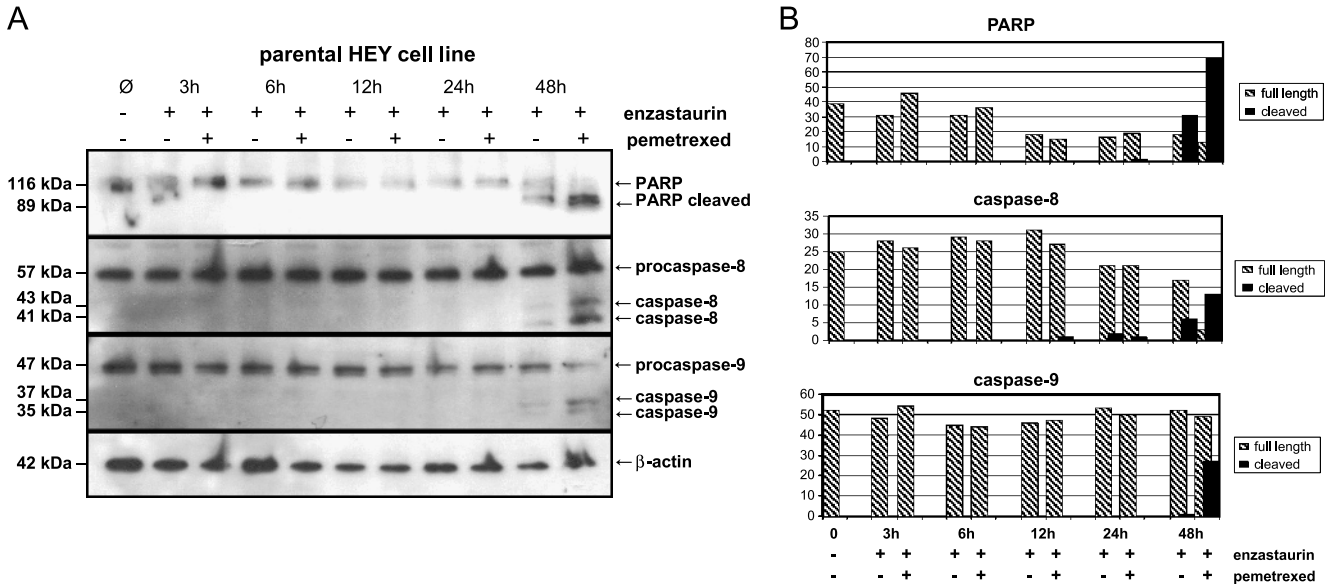

Figure 5. Effects of cotreatment of enzastaurin and pemetrexed on the proapoptotic proteins PARP, caspase 8, and caspase 9. (A) Parental HEY cells were treated with both 10 μM enzastaurin and 10 μM enzastaurin plus 50 nM pemetrexed for the indicated times, and cleavage in the proapoptotic active forms was determined by immunoblot experiments with the appropriate antibodies. Expression analysis of β-actin served as loading control. (B) Histograms show densitometrical analyses of the full length and cleaved amount of PARP, caspase 8, and caspase 9 normalized to the protein expression of β-actin.

enzastaurin treatment. As also described in other studies, the IC_{50} values varied greatly [32,33]. The strongest sensitivity is displayed by the cisplatin-resistant cell line, which responded even more clearly to enzastaurin than the parental HEYs. This is interesting because platinum resistance in ovarian carcinoma is correlated with bad prognosis and seemed to be partially overcome by enzastaurin stimulation *in vitro*. In contrast, 16 μM enzastaurin was needed to inhibit 50% of proliferation in the docetaxel-resistant cells. Little is known about cross resistances with enzastaurin; Lee et al. [33] described enzastaurin-dependent induction of apoptosis in gastric cancer cell lines and additive or synergistic effects after combined treatment with either cisplatin or paclitaxel.

To evaluate the different responses to enzastaurin treatment in the parental and cytostatic-resistant cell lines, the known targets of enzastaurin PKCβII and GSK3β were investigated. Similar to a previous work [34], the amount of both activated and total PKCβII protein did not correlate with chemosensitivity to enzastaurin, neither in untreated (Figure W1) nor in enzastaurin-treated cells (data not shown). In line with previous observations, we also detected dephosphorylation of GSK3β already after 30 minutes of enzastaurin treatment in the parental and the chemoresistant cell lines (Figure 2). Furthermore, we could demonstrate that dephosphorylation and thus activation of GSK3β correlates with the enzastaurin-induced proliferation inhibition: The most enzastaurin-sensitive cisplatin-resistant subclone showed the strongest GSK3β dephosphorylation, whereas the more resistant docetaxel-resistant cell line displayed less dephosphorylation of GSK3β. Enzastaurin-caused dephosphorylation of GSK3β was mostly linked to the PI3K/AKT pathway. Down-regulation of AKT and GSK3β was apparent at the same treatment periods [23,34]. In our study, expression of phosphorylated AKT also showed a distinct decrease with enzastaurin but only after 48 hours of stimulation. Rizvi et al. [25], who made the same observation, explained that the loss of inactive GSK3β at an earlier time point may have been due to PKC inhibition alone. Graff et al. [23] also described a delay of dephosphorylation of AKT relative to enzastaurin-caused inhibition of GSK3β phosphorylation, but in contrast to our results, they showed a dephosphorylation of AKT already after 4 hours. Another indicator of the different regulation in our ovarian cancer cell line is the persisting dephosphorylation of GSK3β after 48 hours of enzastaurin treatment compared with untreated cells. In xenograft tissue samples, a time-dependent suppression of phosphorylated GSK3β up to 8 hours was described, which returned to pretreatment levels after 12 hours of dosing [23]. Our ovarian cancer cell line showed the strongest dephosphorylation of GSK3β after 12 hours of enzastaurin exposition resembling the observation we investigated for enzastaurin-caused dephosphorylation of the MAP kinase ERK1/2 (Figure 6). This is consistent with earlier studies that suggest that activation of ERK1/2 can also phosphorylate GSK3β and promote cell survival in addition to the PI3K/AKT pathway [35,36]. Previous reports demonstrated that a PKC activator phorbol 12-myristate 13-acetate increased prostaglandin E_2 release resulting in activation of PKCβ, ERKs, and p38 MAP kinase in murine macrophages [37]. Furthermore, Langford et al. [38] suggested a cross talk between GSK3β and ERK1/2 that is possibly mediated by PKC in fibroblast growth factor 2–stimulated human umbilical vein endothelial cells. Recently, some studies have focused on how PKCβ collaborates with MAP kinase signaling pathways to regulate cell survival and cell death [39,40]. Our study demonstrated a distinct enzastaurin-dependent regulation of the ERK1/2 pathway with a concordant phosphorylation pattern, as shown for GSK3β. Consistent with these findings, Podar et al. [24] determined that enzastaurin specifically inhibits 12-*O*-tetradecanoyl-phorbol-13-acetate–triggered phosphorylation of signaling molecules downstream of PKC, namely, GSK3β and ERK1/2. Concordant with our findings, Guo et al. [41] revealed the important role of the PKCβ/ERK1/2 pathway: Both the selective PKCβII inhibitor enzastaurin and PKCβII small interfering RNA decreased the phosphorylation of ERK1/2 in metastatic

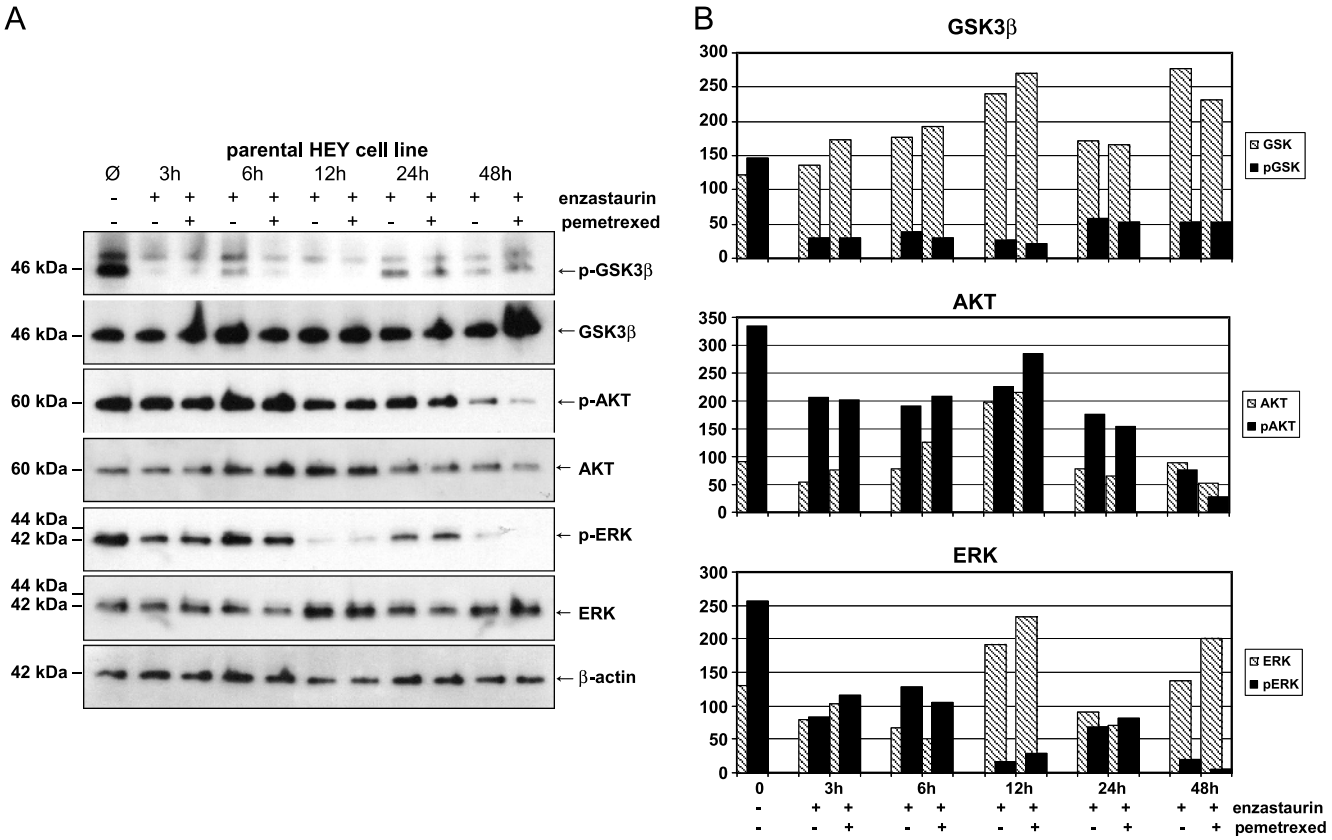

Figure 6. Effects of cotreatment of enzastaurin and pemetrexed on the proproliferative kinases GSK3β, AKT, and ERK1/2. (A) Parental HEY cells were treated with both 10 μM enzastaurin and 10 μM enzastaurin plus 50 nM pemetrexed for indicated times. Phosphorylation and total protein amount of GSK3β, AKT, and ERK1/2 were determined by immunoblot experiments with the appropriate antibodies. Expression analysis of β-actin served as loading control. (B) Histograms show densitometrical analyses of the phosphorylated and total amount of the protein expression of GSK3β, AKT, and the MAP kinase ERK1/2 normalized to the protein expression of β-actin.

hepatocellular carcinoma cell lines. Our observation of the slight increase of ERK1/2 phosphorylation after 24 hours of drug treatment may contribute to growth proliferation being a sort of mechanism that cancer cells use to escape drug-induced death.

Because enzastaurin only partially inhibited the proliferation of our ovarian cancer cell lines at clinically achievable concentrations, cotreatment with the multitargeted antifolate pemetrexed was supposed to enhance enzastaurin-induced effects. Pemetrexed is well tolerated and has been associated with a significant reduction of phosphorylated AKT as well as a synergistic antiproliferative effect in combination treatment with gemcitabine in human NSCLC cells [29]. Given in combination with cisplatin, pemetrexed has recently been approved for the treatment of malignant pleural mesothelioma and as a second-line treatment of NSCLC [42]. In our study, we could prove a synergistic proliferation inhibition in the parental and all drug-resistant HEY cell lines by concomitant treatment of enzastaurin and pemetrexed. Even the docetaxel-resistant HEY cells, which displayed a partial enzastaurin as well as pemetrexed resistance, were affected by this combination.

Apoptosis induction was investigated by PARP and caspase cleavage analyses and confirmed a synergistic effect of cotreatment in the parental HEY cell line. Partial PARP cleavage occurred after 48 hours of enzastaurin treatment. Combined treatment with pemetrexed resulted in nearly completely cleaved PARP, demonstrating increased induction of apoptosis. Investigation of the initiator caspases 8 and 9 also displayed a slight cleavage into the proapoptotic active proteins by enzastaurin exposition, which was additionally enforced by concomitant administration of pemetrexed. The apoptotic induction by enzastaurin was mediated through the activation of caspase 9 in the parental ovarian cancer cell line HEY, where an enzastaurin-resistant control cell line showed no caspase 9 cleavage after enzastaurin treatment (Figure W2). Cleavage of caspase 8 could be detected in both cell lines. This observation suggests that the mitochondrial apoptotic pathway is involved in enzastaurin-induced ovarian cancer cell death. Similar results were described by Rieger et al. [43] in glioma cell lines. They showed that enzastaurin-induced apoptosis involved cleavage of both caspases 8 and 9, which was strongly suppressed by the common caspase inhibitor zVAD-fmk but only slightly by the expression of a special caspase 8 inhibitor.

In 2005, Oberschmidt et al. [44] already described a synergistic antitumor activity in thyroid cancer cell lines. In contrast, in the studies of Hanauske et al. [45,46], enzastaurin gave no additional activity to pemetrexed after long-term treatment. Morgillo et al. [47] compared sequential with concomitant stimulation in a panel of NSCLC cells and found that only a synergistic antiproliferative and proapoptotic activity was obtained when pemetrexed was followed by treatment of enzastaurin. In their study, the concomitant combination treatment caused a decrease in IC_{50} values for the single treatment of enzastaurin in the most enzastaurin-resistant NSCLC cell line Calu-3. We could

prove a similar effect for our docetaxel-resistant cell line. Interestingly, the sequential combination treatment, which led to synergistic antiproliferative and proapoptotic activity in this study, also resulted in enhanced dephosphorylation of ERK1/2 and AKT. Our observations also showed synergistic antiproliferative and proapoptotic effects by concordant treatment in the ovarian cancer cell line HEY, which are associated with the enhanced inhibition of the proproliferative kinases ERK1/2 and AKT. Moreover, the recently published investigation of Tekle et al. [48] revealed strong synergistic effects by cotreatment of enzastaurin and pemetrexed in simultaneous treatment as well as in the sequential schedule in NSCLC cells. Similar to our results, a further decrease of phosphorylation of AKT by simultaneous cotreatment could be observed. Although the drug combination showed enhancement of phosphorylated ERK1/2 in the investigation of Tekle et al. [48], single treatment with enzastaurin displayed a strong decrease in the activated MAP kinase, confirming our results.

Conclusions

In the present study, we showed that enzastaurin exhibited direct antitumor activity, inducing tumor cell apoptosis and suppressing tumor cell proliferation in the ovarian cancer cell line HEY and in the chemoresistant subclones, most prominent in the cisplatin-resistant HEYs. Besides influencing its target GSK3β, enzastaurin interferes with signaling mainly through the ERK1/2 pathway, a pathway frequently activated in a variety of human cancers, and the AKT pathway. In addition, we could demonstrate a synergistic antiproliferative and proapoptotic effect by the combined treatment with enzastaurin and pemetrexed. This combination treatment also causes inhibition of proliferation in partial enzastaurin-resistant cells at achievable clinical concentrations with the most promising effect in the docetaxel-resistant HEYs. Therefore, this combination warrants clinical testing to overcome chemotherapy resistance in ovarian cancer.

Acknowledgments

The authors thank Dawn Rüther for reading and correcting the manuscript.

References

[1] Jemal A, Siegel R, Ward E, Hao Y, Xu J, Murray T, and Thun MJ (2008). Cancer statistics, 2008. *CA Cancer J Clin* **58**, 71–96.

[2] Memarzadeh S and Berek JS (2001). Advances in the management of epithelial ovarian cancer. *J Reprod Med* **46**, 621–629; discussion 629–630.

[3] Salani R, Santillan A, Zahurak ML, Giuntoli RL II, Gardner GJ, Armstrong DK, and Bristow RE (2007). Secondary cytoreductive surgery for localized, recurrent epithelial ovarian cancer: analysis of prognostic factors and survival outcome. *Cancer* **109**, 685–691.

[4] Neijt JP, Engelholm SA, Tuxen MK, Sorensen PG, Hansen M, Sessa C, de Swart CA, Hirsch FR, Lund B, and van Houwelingen HC (2000). Exploratory phase III study of paclitaxel and cisplatin *versus* paclitaxel and carboplatin in advanced ovarian cancer. *J Clin Oncol* **18**, 3084–3092.

[5] Martiny-Baron G and Fabbro D (2007). Classical PKC isoforms in cancer. *Pharmacol Res* **55**, 477–486.

[6] Griner EM and Kazanietz MG (2007). Protein kinase C and other diacylglycerol effectors in cancer. *Nat Rev Cancer* **7**, 281–294.

[7] Nishizuka Y (1995). Protein kinase C and lipid signaling for sustained cellular responses. *FASEB J* **9**, 484–496.

[8] Xia P, Aiello LP, Ishii H, Jiang ZY, Park DJ, Robinson GS, Takagi H, Newsome WP, Jirousek MR, and King GL (1996). Characterization of vascular endothelial growth factor's effect on the activation of protein kinase C, its isoforms, and endothelial cell growth. *J Clin Invest* **98**, 2018–2026.

[9] Goekjian PG and Jirousek MR (2001). Protein kinase C inhibitors as novel anticancer drugs. *Expert Opin Investig Drugs* **10**, 2117–2140.

[10] Clark JA, Black AR, Leontieva OV, Frey MR, Pysz MA, Kunneva L, Woloszynska-Read A, Roy D, and Black JD (2004). Involvement of the ERK signaling cascade in protein kinase C–mediated cell cycle arrest in intestinal epithelial cells. *J Biol Chem* **279**, 9233–9247.

[11] Greco S, Storelli C, and Marsigliante S (2006). Protein kinase C (PKC)-δ/ε mediate the PKC/Akt–dependent phosphorylation of extracellular signal–regulated kinases 1 and 2 in MCF-7 cells stimulated by bradykinin. *J Endocrinol* **188**, 79–89.

[12] Zhang J, Anastasiadis PZ, Liu Y, Thompson EA, and Fields AP (2004). Protein kinase C (PKC) βII induces cell invasion through a Ras/Mek–, PKC iota/Rac 1–dependent signaling pathway. *J Biol Chem* **279**, 22118–22123.

[13] Aeder SE, Martin PM, Soh JW, and Hussaini IM (2004). PKC-η mediates glioblastoma cell proliferation through the Akt and mTOR signaling pathways. *Oncogene* **23**, 9062–9069.

[14] Balendran A, Hare GR, Kieloch A, Williams MR, and Alessi DR (2000). Further evidence that 3-phosphoinositide–dependent protein kinase-1 (PDK1) is required for the stability and phosphorylation of protein kinase C (PKC) isoforms. *FEBS Lett* **484**, 217–223.

[15] Partovian C and Simons M (2004). Regulation of protein kinase B/Akt activity and Ser473 phosphorylation by protein kinase Cα in endothelial cells. *Cell Signal* **16**, 951–957.

[16] Kawakami Y, Nishimoto H, Kitaura J, Maeda-Yamamoto M, Kato RM, Littman DR, Leitges M, Rawlings DJ, and Kawakami T (2004). Protein kinase CβII regulates Akt phosphorylation on Ser-473 in a cell type– and stimulus-specific fashion. *J Biol Chem* **279**, 47720–47725.

[17] Fang X, Yu S, Tanyi JL, Lu Y, Woodgett JR, and Mills GB (2002). Convergence of multiple signaling cascades at glycogen synthase kinase 3: Edg receptor–mediated phosphorylation and inactivation by lysophosphatidic acid through a protein kinase C–dependent intracellular pathway. *Mol Cell Biol* **22**, 2099–2110.

[18] Goode N, Hughes K, Woodgett JR, and Parker PJ (1992). Differential regulation of glycogen synthase kinase-3β by protein kinase C isotypes. *J Biol Chem* **267**, 16878–16882.

[19] Cross DA, Alessi DR, Cohen P, Andjelkovich M, and Hemmings BA (1995). Inhibition of glycogen synthase kinase-3 by insulin mediated by protein kinase B. *Nature* **378**, 785–789.

[20] Hersey P, Zhuang L, and Zhang XD (2006). Current strategies in overcoming resistance of cancer cells to apoptosis melanoma as a model. *Int Rev Cytol* **251**, 131–158.

[21] Faul MM, Gillig JR, Jirousek MR, Ballas LM, Schotten T, Kahl A, and Mohr M (2003). Acyclic *N*-(azacycloalkyl)bisindolylmaleimides: isozyme selective inhibitors of PKCβ. *Bioorg Med Chem Lett* **13**, 1857–1859.

[22] Keyes KA, Mann L, Sherman M, Galbreath E, Schirtzinger L, Ballard D, Chen YF, Iversen P, and Teicher BA (2004). LY317615 decreases plasma VEGF levels in human tumor xenograft-bearing mice. *Cancer Chemother Pharmacol* **53**, 133–140.

[23] Graff JR, McNulty AM, Hanna KR, Konicek BW, Lynch RL, Bailey SN, Banks C, Capen A, Goode R, Lewis JE, et al. (2005). The protein kinase Cβ–selective inhibitor, enzastaurin (LY317615.HCl), suppresses signaling through the AKT pathway, induces apoptosis, and suppresses growth of human colon cancer and glioblastoma xenografts. *Cancer Res* **65**, 7462–7469.

[24] Podar K, Raab MS, Zhang J, McMillin D, Breitkreutz I, Tai YT, Lin BK, Munshi N, Hideshima T, Chauhan D, et al. (2007). Targeting PKC in multiple myeloma: *in vitro* and *in vivo* effects of the novel, orally available small-molecule inhibitor enzastaurin (LY317615.HCl). *Blood* **109**, 1669–1677.

[25] Rizvi MA, Ghias K, Davies KM, Ma C, Weinberg F, Munshi HG, Krett NL, and Rosen ST (2006). Enzastaurin (LY317615), a protein kinase Cβ inhibitor, inhibits the AKT pathway and induces apoptosis in multiple myeloma cell lines. *Mol Cancer Ther* **5**, 1783–1789.

[26] Carducci MA, Musib L, Kies MS, Pili R, Truong M, Brahmer JR, Cole P, Sullivan R, Riddle J, Schmidt J, et al. (2006). Phase I dose escalation and pharmacokinetic study of enzastaurin, an oral protein kinase Cβ inhibitor, in patients with advanced cancer. *J Clin Oncol* **24**, 4092–4099.

[27] Chattopadhyay S, Moran RG, and Goldman ID (2007). Pemetrexed: biochemical and cellular pharmacology, mechanisms, and clinical applications. *Mol Cancer Ther* **6**, 404–417.

[28] Adjei AA (2004). Pemetrexed (ALIMTA), a novel multitargeted antineoplastic agent. *Clin Cancer Res* **10**, 4276s–4280s.

[29] Giovannetti E, Mey V, Nannizzi S, Pasqualetti G, Marini L, Del Tacca M, and Danesi R (2005). Cellular and pharmacogenetics foundation of synergistic interaction of pemetrexed and gemcitabine in human non–small-cell lung cancer cells. *Mol Pharmacol* **68**, 110–118.

[30] Adjei AA (2006). Clinical studies of pemetrexed and gemcitabine combinations. *Ann Oncol* **17** (Suppl 5), v29–v32.

[31] Smith I (2004). Phase II studies of pemetrexed in metastatic breast and gynecologic cancers. *Oncology (Williston Park)* **18**, 63–65.

[32] Jane EP and Pollack IF (2008). The heat shock protein antagonist 17-AAG potentiates the activity of enzastaurin against malignant human glioma cells. *Cancer Lett* **268**, 46–55.

[33] Lee KW, Kim SG, Kim HP, Kwon E, You J, Choi HJ, Park JH, Kang BC, Im SA, Kim TY, et al. (2008). Enzastaurin, a protein kinase Cβ inhibitor, suppresses signaling through the ribosomal S6 kinase and bad pathways and induces apoptosis in human gastric cancer cells. *Cancer Res* **68**, 1916–1926.

[34] Querfeld C, Rizvi MA, Kuzel TM, Guitart J, Rademaker A, Sabharwal SS, Krett NL, and Rosen ST (2006). The selective protein kinase Cβ inhibitor enzastaurin induces apoptosis in cutaneous T-cell lymphoma cell lines through the AKT pathway. *J Invest Dermatol* **126**, 1641–1647.

[35] Eldar-Finkelman H, Seger R, Vandenheede JR, and Krebs EG (1995). Inactivation of glycogen synthase kinase-3 by epidermal growth factor is mediated by mitogen-activated protein kinase/p90 ribosomal protein S6 kinase signaling pathway in NIH/3T3 cells. *J Biol Chem* **270**, 987–990.

[36] Stambolic V and Woodgett JR (1994). Mitogen inactivation of glycogen synthase kinase-3β in intact cells via serine 9 phosphorylation. *Biochem J* **303** (Pt 3), 701–704.

[37] Lin WW and Chen BC (1999). Induction of cyclo-oxygenase-2 expression by methyl arachidonyl fluorophosphonate in murine J774 macrophages: roles of protein kinase C, ERKs and p38 MAPK. *Br J Pharmacol* **126**, 1419–1425.

[38] Langford D, Hurford R, Hashimoto M, Digicaylioglu M, and Masliah E (2005). Signalling crosstalk in FGF2-mediated protection of endothelial cells from HIV-gp120. *BMC Neurosci* **6**, 8.

[39] Troller U, Zeidman R, Svensson K, and Larsson C (2001). A PKCβ isoform mediates phorbol ester–induced activation of Erk1/2 and expression of neuronal differentiation genes in neuroblastoma cells. *FEBS Lett* **508**, 126–130.

[40] Fujita T, Asai T, Andrassy M, Stern DM, Pinsky DJ, Zou YS, Okada M, Naka Y, Schmidt AM, and Yan SF (2004). PKCβ regulates ischemia/reperfusion injury in the lung. *J Clin Invest* **113**, 1615–1623.

[41] Guo K, Liu Y, Zhou H, Dai Z, Zhang J, Sun R, Chen J, Sun Q, Lu W, Kang X, et al. (2008). Involvement of protein kinase Cβ–extracellular signal–regulating kinase 1/2/p38 mitogen-activated protein kinase–heat shock protein 27 activation in hepatocellular carcinoma cell motility and invasion. *Cancer Sci* **99**, 486–496.

[42] Pearce HL and Alice Miller M (2005). The evolution of cancer research and drug discovery at Lilly Research Laboratories. *Adv Enzyme Regul* **45**, 229–255.

[43] Rieger J, Lemke D, Maurer G, Weiler M, Frank B, Tabatabai G, Weller M, and Wick W (2008). Enzastaurin-induced apoptosis in glioma cells is caspase-dependent and inhibited by BCL-XL. *J Neurochem* **106**, 2436–2448.

[44] Oberschmidt O, Eismann U, Schulz L, Struck S, Blatter J, Lahn MM, Ma D, and Hanauske AR (2005). Enzastaurin and pemetrexed exert synergistic antitumor activity in thyroid cancer cell lines *in vitro*. *Int J Clin Pharmacol Ther* **43**, 603–604.

[45] Hanauske AR, Oberschmidt O, Hanauske-Abel H, Lahn MM, and Eismann U (2007). Antitumor activity of enzastaurin (LY317615.HCl) against human cancer cell lines and freshly explanted tumors investigated in *in-vitro* [corrected] soft-agar cloning experiments. *Invest New Drugs* **25**, 205–210.

[46] Hanauske AR, Eismann U, Oberschmidt O, Pospisil H, Hanauske-Abel HM, Blatter J, Ma D, Chen V, and Lahn M (2008). Correlations of mRNA expression and *in vitro* chemosensitivity to enzastaurin in freshly explanted human tumor cells. *Invest New Drugs* **26**, 215–222.

[47] Morgillo F, Martinelli E, Troiani T, Laus G, Pepe S, Gridelli C, and Ciardiello F (2008). Sequence-dependent, synergistic antiproliferative and proapoptotic effects of the combination of cytotoxic drugs and enzastaurin, a protein kinase Cβ inhibitor, in non–small cell lung cancer cells. *Mol Cancer Ther* **7**, 1698–1707.

[48] Tekle C, Giovannetti E, Sigmond J, Graff JR, Smid K, and Peters GJ (2008). Molecular pathways involved in the synergistic interaction of the PKCβ inhibitor enzastaurin with the antifolate pemetrexed in non–small cell lung cancer cells. *Br J Cancer* **99**, 750–759.

Table W1. Determination of IC_{50} Values of Appropriate Cytostatic Drugs in the Parental and Chemoresistant HEY Cell Lines.

IC_{50}	Cisplatin	Etoposide	Docetaxel	Paclitaxel	Pemetrexed	Gemcitabine	Enzastaurin
Parental HEYs	0.7 μg/ml	0.5 μg/ml	1.4 ng/ml	3.4 ng/ml	0.06 μM	0.1 μM	8.6 μM
Cisplatin HEYs	7.5 μg/ml						
Etoposide HEYs		78.8 μg/ml					
Docetaxel HEYs			76.3 ng/ml				
Paclitaxel HEYs				453.0 ng/ml			
Pemetrexed HEYs					336.2 μM		
Gemcitabine HEYs						19.8 μM	
Enzastaurin HEYs							29.4 μM

The parental HEY cells and the cytostatic drug-resistant subclones were treated with rising concentrations of the subsequent drugs and the appropriate IC_{50} values were investigated by MTS assay from Promega.

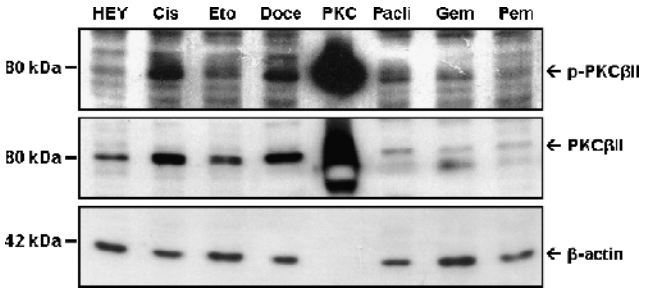

Figure W1. Differences in PKCβII protein expression determined by immunoblot analysis of total cell protein extracts in untreated parental and drug-resistant HEYs. The expression level of phosphorylated PKCβII resembled the total amount of PKCβII. Analyses of β-actin served as loading control. *HEY* indicates parental HEY cell line; *Cis*, cisplatin-resistant HEY cell line; *Eto*, etoposide-resistant HEY cell line; *Doce*, docetaxel-resistant HEY cell line; *Pacli*, paclitaxel-resistant HEY cell line; *Gem*, gemcitabine-resistant HEY cell line; *Pem*, pemetrexed-resistant HEY cell line; *PKC*, PKCβII peptide, positive control.

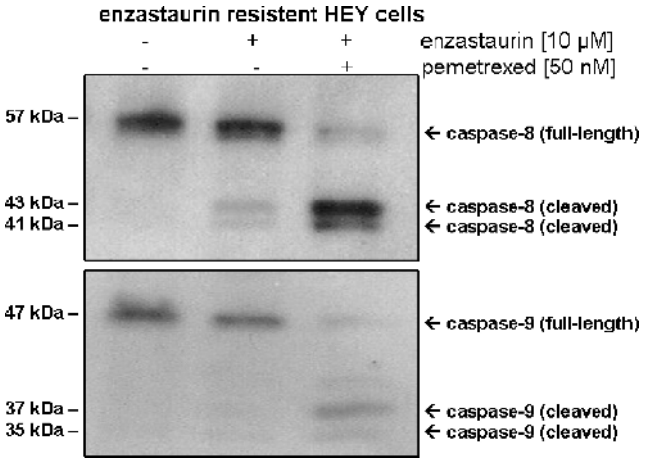

Figure W2. Enzastaurin-resistant cells were treated with both 10 μM enzastaurin and the combination of 10 μM enzastaurin and 50 nM pemetrexed for 48 hours. Cleavage of caspases 8 and 9 was determined by immunoblot analyses.